The Road to the Artemis Base Camp Via Applied Science: Estimating the Bulk Density of Lunar Regolith Stratigraphy Through Cone Penetrometer Testing of Simulants

Michael P. Lucas[1], Clive R. Neal[1], Jared Long-Fox[2], and Daniel Britt[2], [1]Dept. of Civil & Environmental Engineering & Earth Sciences, University of Notre Dame, mlucas25@nd.edu, [2]Dept. of Physics, University of Central Florida.

Motivation: The geotechnical properties of lunar simulants have remained largely uncharacterized. Given the profusion of existing simulants [see 1], plus many new simulant formulations being prepared for analogue investigations to enable lunar exploration, the planetary-surface simulant community is presently undergoing an era of "wild-west" development and expansion. Therefore, it is imperative that new and existing simulants undergo rigorous geotechnical characterization in order to understand how to calibrate in situ testing on the Moon that will be required to guide future lunar regolith excavation, construction, and mining activities.

Introduction: Geotechnical measurements conducted during the Apollo missions showed that the density of near-surface regolith layers significantly increases with depth [2,3]. In fact, in situ cone penetrometer testing (CPT) measurements (also drive tube & drill stem samples) at Apollo 16 Stations 4 & 10 showed that a firm layer is encountered at 5–10 cm below the surface and that relative density increases to >90% at depths of 20–40 cm [4]. These observations emphasize an often-overlooked aspect regarding lunar regolith/lunar simulant comparisons; to understand how the regolith can enable, but must withstand, construction activities, it will be critical to understand the geotechnical properties and density profile of the near-surface lunar regolith while performing large-scale engineering tests (i.e., pack simulant in layers of specific densities, rather than just dumping it into the test bed [5]). Here, we use Exolith Lab lunar simulants to develop geotechnical correlations between CPT measurements and bulk density (ρ_B) that are crucial for future lunar infrastructure development (e.g., launch/landing pad - LLP), and other base logistics, such as vehicle trafficability and ISRU activities.

Cone Penetrometer Measurements: We used a Rimik CP40II penetrometer to obtain Cone Index (CI) penetration resistance values (stress in kPa) vs. depth for lunar simulants packed at various ρ_B in clear, acrylic test bins (~30×30×80 cm tall) (Fig. 1). We used an ASAE standard cone area of 1.29 cm^2 [6], the same as that used for CPT measurements during the Apollo 16 mission (but not Apollo 15, which used only a 3.22 cm^2 cone). We measured CI values at 10 mm intervals to depths of ~150-200 mm to estimate the slope parameter (G), which is the slope of CI values vs. depth measured from the surface to 100 mm depth [see 5,7].

Slope Parameter Derivation for Lunar Simulants: To derive geotechnical correlations between CPT data and ρ_B, we measured CI values of simulants packed at specific densities to determine their range of strength in terms of G. We developed correlations for three variations of

Figure 1. Rimik CP40II CPT insertion into LHS-1B "Simplified" lunar highlands simulant column packed within a clear, acrylic test bin at ρ_B = 1.83 g/cm^3 (12" ruler for scale).

LHS-1 lunar highlands simulant (see [8] for geotechnical properties): LHS-1-D (D=dried at ~110±5 °C for ~4 hr and stored in airtight containers), LHS-1-U (U=undried; moisture content ~820±100 ppm; n=9), and LHS-1B Undried (moisture content ~770±110 ppm; n=12; defined as LHS-1B-U) (Fig. 2). LHS-1B is designed to be a simplified, lower-cost alternative simulant applicable for large-scale engineering tests and is essentially LHS-1 minus the trace minerals (e.g., ilmenite, olivine, and pyroxene). We also developed a correlation for lunar mare simulant LMS-1 Undried (see [9] for geotechnical properties; moisture content ~2900±370 ppm; n=11; defined as LMS-1-U) (Fig. 3). Moisture contents were measured using ASTM standards [10]. Specific ρ_B values were achieved through vibration and by applying variable surcharge loads to the surface of the simulant column. G was determined over a range of densities to derive correlations between G and ρ_B for the lunar simulant variations (Figs. 2 and 3). G values for LHS-1-D, LHS-1-U, and LHS-1B-U are in good agreement with the range of estimated G values determined from highland CPT data at Apollo 16 Stations 4 & 10 (Fig. 2). However, estimated G values from CPT data at the Apollo 15 mare landing site were obtained using a 3.22 cm^2 cone and are not directly comparable to our LMS-1-U CPT data (see Fig. 3). All four data sets yield strong exponential relationships (R^2 values of 0.92 to 0.98; Figs. 2 & 3; log y-axis), which were fitted using the least squares method. These relationships are described by the following equations (solved for ρ_B):

LHS-1-D: $\rho_B = (\ln G + 16.6)/10.524$ (Eq. 1)

LHS-1-U: $\rho_B = (\ln G + 13.2)/8.451$ (Eq. 2)

LHS-1B-U: $\rho_B = (\ln G + 15.8)/9.934$ (Eq. 3)

LMS-1-U: $\rho_B = (\ln G + 15.9)/8.978$ (Eq. 4)

The exponential relationships between G and ρ_B found here are in contrast with the linear trend found for the geomechanical simulant GRC-1, which was derived using much lower densities than measured in this study (see Fig. 6 in [10]).

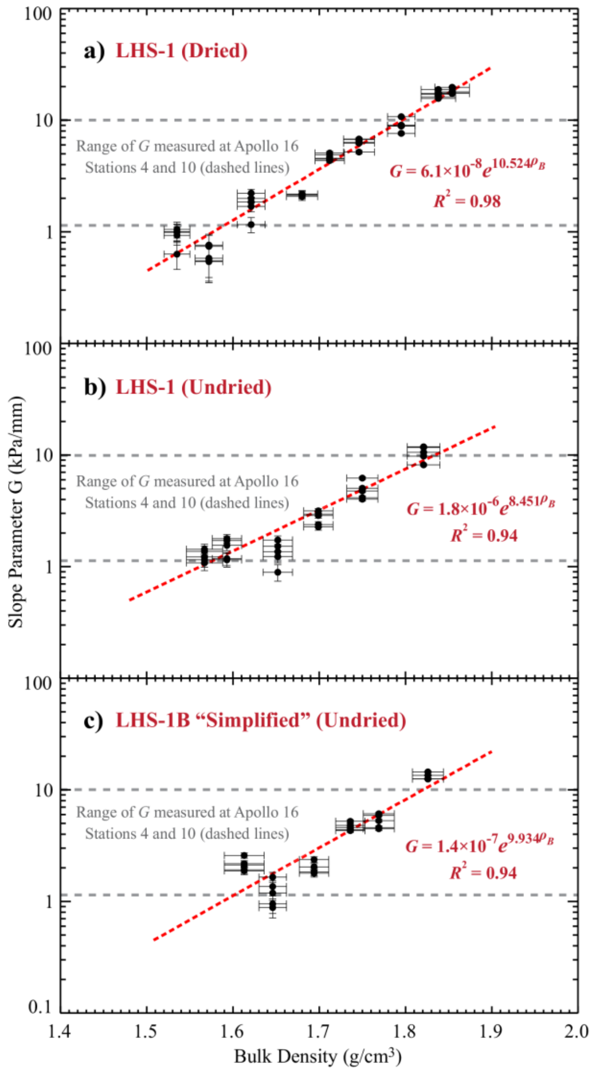

Figure 2. Slope parameter (G; log scale) of stress-penetration curves vs. ρ_B for three variations of LHS-1 highland lunar simulant. Data (black circles) for **(a)** LHS-1-D (45 G values), **(b)** LHS-1-U (30 G values), **(c)** LHS-1B-U (29 G values), yield strong exponential relationships.

Statistical Comparison of G-slope Correlations: To quantify how our G-slope correlations compare to each other we used Eqs. 1-4 to produce four sets of predicted ρ_B values (n=35 each). We then employed two statistical tests to compare these data sets. The two-sample Kolmogorov-Smirnov (K-S) test is used to test for significant differences and to calculate the maximum difference (D) between two distributions, while the Mann-Whitney (M-W) U test is used to test for significant differences in medians (central tendency) between two distributions. Both statistical tests are performed under the

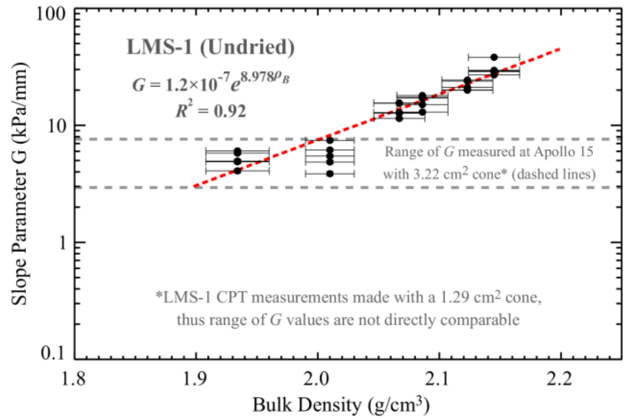

Figure 3. Slope parameter (G; log scale) of stress-penetration curves vs. ρ_B for LMS-1-U mare lunar simulant (30 G values). The data (black circles) yield a strong exponential relationship.

null hypothesis that the bulk density predictions are drawn from identical distributions using a significance level of α=0.05 (95% confidence). Table 1 indicates that the null hypothesis is rejected for LHS-1-U vs. LMS-1-U; predicted ρ_B for these two simulants are significantly different at the 95% confidence level, while p-values for LHS-1-U vs. LHS-1B-U are statistically indistinguishable at the 95% confidence level. Although the null hypothesis is not rejected for LHS-1-D vs. LHS-1-U, **low p-values suggest that dried simulants are better analogues for the lunar surface than undried simulants.**

Table 1. Two-sample Kolmogorov-Smirnov (K-S) and Mann-Whitney (M-W) U test results (n = 35 for each sample)

Parameter	D_α	D	U	*p-value*
LHS-1 (dried) versus LHS-1 (undried)				
K-S distribution (D)	0.33	0.28	-	12%
M-W central tend. (U)	-	-	468	9%
LHS-1 (undried) versus LHS-1B "simplified" (undried)				
K-S distribution	0.33	0.17	-	69%
M-W central tend. (U)	-	-	672	48%
LHS-1 (undried) versus LMS-1 (undried)				
K-S distribution	0.33	0.74	-	1×10^{-7}%
M-W central tend. (U)	-	-	112	4×10^{-7}%

D_α - null hypothesis is rejected if D is $>D_\alpha$
U – maximum value of U is the product of the two sample sizes; for this study U_{max} = 1225
p-value – probability of the two-sample data being drawn from identical distributions (K-S) or having the same central tendency (M-W)

Future Work: Future work includes the development of G-slope vs. density correlations for all Exolith Lab lunar and martian simulants.

References: [1] NASA-ARES (2022) Astromaterials Res. & Exploration https://ares.jsc.nasa.gov/projects/simulants/. [2] Carrier et al. (1991) *Lunar Sourcebook*, Chap. 9. [3] Carrier (2005) *LPI Technical Report.* [4] Mitchell et al. (1972) *Apollo 16 Prelim Sci. Report*, Chap. 8. [5] Lucas et al. (2023) *Acta Astronautica, in review*. [6] ASAE S313.3 (1999) *Soil Cone Penetrometer.* [7] Houston and Namiq (1971) *Journal of Terramechanics* 8, 59-69. [8] Long-Fox et al. (2022) *ASCE Earth & Space Proceedings*. [9] Long-Fox et al. (2023) *Advances in Space Research, in review.* [10] ASTM International (2019) D2216-19. [11] Oravec et al. (2010) *Journal of Terramechanics* 47, 361-377.